H_2-induced transient upregulation of phospholipids with suppression of energy metabolism

Masumi Iketani[1, #], Iwao Sakane[1, 2, #], Yasunori Fujita[1], Masafumi Ito[1], Ikuroh Ohsawa[1, *]
1 Biological Process of Aging, Tokyo Metropolitan Institute of Gerontology, Tokyo, Japan
2 Central Research Institute, ITO EN Ltd., Shizuoka, Japan

*Correspondence to: Ikuroh Ohsawa, PhD, iohsawa@tmig.or.jp.
#Both authors contributed equally to this work.
orcid: 0000-0002-7212-9298 (Ikuroh Ohsawa)

Abstract

Molecular hydrogen (H_2) is an antioxidant and anti-inflammatory agent; however, the molecular mechanisms underlying its biological effects are largely unknown. Similar to other gaseous molecules such as inhalation anesthetics, H_2 is more soluble in lipids than in water. A recent study demonstrated that H_2 reduces radical polymerization-induced cellular damage by suppressing fatty acid peroxidation and membrane permeability. Thus, we sought to examine the effects of short exposure to H_2 on lipid composition and associated physiological changes in SH-SY5Y neuroblastoma cells. We analyzed cells by liquid chromatography-high-resolution mass spectrometry to define changes in lipid components. Lipid class analysis of cells exposed to H_2 for 1 hour revealed transient increases in glycerophospholipids including phosphatidylethanolamine, phosphatidylinositol, and cardiolipin. Metabolomic analysis also showed that H_2 exposure for 1 hour transiently suppressed overall energy metabolism accompanied by a decrease in glutathione. We further observed alterations to endosomal morphology by staining with specific antibodies. Endosomal transport of cholera toxin B to recycling endosomes localized around the Golgi body was delayed in H_2-exposed cells. We speculate that H_2-induced modification of lipid composition depresses energy production and endosomal transport concomitant with enhancement of oxidative stress, which transiently stimulates stress response pathways to protect cells.

Key words: cultured cells; endosome; gas; glutathione; lipid composition; metabolome; molecular hydrogen; neuroblastoma; oxidative stress; phospholipid

doi: 10.4103/2045-9912.344973
How to cite this article: Iketani M, Sakane I, Fujita Y, Ito M, Ohsawa I. H_2-induced transient upregulation of phospholipids with suppression of energy metabolism. Med Gas Res. 2023;13(3):133-141.
Funding: This work is supported by the Japan Society for the Promotion of Science (JSPS) Grant-in-Aid for Scientific Research (KAKENHI) (B) 20H04136 (to IO) and (C) 18K11092 (to MIketani).

Introduction

Molecular hydrogen (H_2) is an antioxidative and antiinflammatory agent. Inhalation of H_2 gas markedly suppresses ischemia/reperfusion injury in several organs by buffering oxidative stress.[1,2] Drinking H_2 dissolved in water is potentially useful to alleviate neurodegenerative diseases, including Parkinson's disease[3] and Alzheimer's disease,[4] and could thus improve the quality of life of elderly people.[5] In animal models, administration of H_2 suppresses inflammatory noncommunicable diseases induced by lipopolysaccharide,[6-8] concanavalin A,[9] and dextran sodium sulfate[10,11] with concomitant decreases in the levels of proinflammatory cytokines. However, the antioxidative, antiinflammatory, and other therapeutic effects of H_2 cannot be completely explained by scavenging of reactive oxygen species because H_2 has a poor ability to reduce them directly.[1,12] On the other hand, animal studies showed that preadministration of H_2 protects against inflammatory diseases.[8,13] We further showed that exposure of cultured cells to H_2 induces mild oxidative stress in mitochondria and subsequent expression of antioxidative enzymes.[14] These results indicate that H_2 triggers mitohormesis, a protective adaptive response against oxidative stress mediated by mitochondria. To determine the precise molecular mechanism underlying the biological effects of H_2, the biomolecules upon which it acts must be identified.

Many gaseous molecules including H_2 are more soluble in lipids than in water.[15] Dissolved gases in lipids affect cellular and physical functions. High concentrations of nitrogen (N_2) increase the bending moduli and stabilities of cellular lipid bilayers and impede phase separation in ternary lipid bilayers.[16] While the precise molecular mechanisms underlying the actions of anesthetics are largely unknown, the Meyer-Overton correlation provides a link between the potency of an anesthetic gas and its solubility in lipid-like non-polar medium. Anesthetic gases dissolved in lipids change cellular membrane structures via hydrophobic interactions.[17] Interestingly, sevoflurane, an inhalation anesthetic, causes brain damage in mice during the developmental period as a side effect, but this damage is reduced by simultaneous inhalation of H_2.[18] Membranes respond rapidly to various environmental perturbations by changing their compositions. For example, exposure to halothane reduces synthesis of phosphatidylcholine (PC), the main lipid component of pulmonary surfactant, in alveolar cells.[19] H_2 was recently reported to reduce the cytotoxic effects of tert-butyl hydroperoxide by suppressing fatty acid peroxidation and membrane permeability,[20] indicating that H_2 affects the membrane environment and lipid composition.

Lipid bilayers, the major constituent of all cellular membranes, are mostly formed by phospholipids. PC, phosphatidylinositol (PI) and phosphatidylserine (PS) mainly promote lipid bilayer formation, whereas the non-bilayer-forming phospholipids, cardiolipin (CL) and

phosphatidylethanolamine (PE), have specific roles in the assembly and activities of mitochondrial respiratory chain complexes.[21] It indicates that cellular metabolism, especially energy production, is significantly affected by the composition change of phospholipids. Furthermore, phospholipids are not passive structural spectators, but actively regulate physiological events such as cytokinesis, exocytosis, and endocytosis.[22] The complex endosomal progression is only partially understood, it is, nevertheless, clear that phospholipids play key functions at various stages of the process. Endocytic vesicles generally fuse with early endosomes (EEs). EEs mature into late endosomes (LEs), which fuse with lysosomes to degrade their contents. Various endocytic pathways have been identified. Some contents, such as the transferrin (Tfn) receptor, are sorted by EEs to recycling endosomes (REs) and returned to the cell membrane.[23] Cholera toxin B (CTxB) is retrogradely transported from REs to the Golgi body.[24]

The present study sought to examine the effects of short exposure to H_2 on lipid composition of cultured human neuroblastoma SH-SY5Y cells because preculture in the presence of H_2 gas for only 3 hours decreases oxidative stress-induced cell death.[14]

Materials and Methods

Cell culture and H_2 exposure

Cells were cultured and exposed to H_2 as previously described.[14] In brief, SH-SY5Y cells (ATCC CRL-2266) were maintained in Dulbecco's modified Eagle medium containing 10% fetal bovine serum, 25 mM 4-(2-hydroxyethyl)-1-piperazineethanesulfonic acid, 1 mM pyruvate, penicillin-streptomycin, and 10 mM glucose. N_2-mixed gas used as a control contained 20% O_2, 5% CO_2, and 75% N_2, which mimicked almost the same condition in acrylamide box (AS ONE, Osaka, Japan) as that in conventional CO_2 incubator. H_2-mixed gas contained 20% O_2, 5% CO_2, and 1–50% H_2 (purity > 99.999%; Iwatani, Tokyo, Japan), with N_2 constituting the remainder. Cells grown for 2 days in a 5% CO_2 incubator on Φ10 cm dishes (2×10^6 cells) for metabolomics, 6-well plates (1×10^6 cells/well) for lipid extraction, 24-well plates (4×10^5 cells/well) for immunoblotting, 96-well plates (4×10^4 cells/well) for the CTxB and Tfn uptake assay, and Φ3.5 cm glass bottom dishes (2×10^5 cells) for immunocytochemistry were set in acrylamide boxes (6.8 L). The boxes were filled with an appropriate mixed gas at a flow rate of 1.6 L/min for 15 minutes under normal pressure, sealed, and put into the incubator at 37°C for the indicated durations. Immediately after incubation, the H_2 and O_2 concentrations in the culture medium were monitored for 15 minutes using specific electrodes (Unisense, Aarhus, Denmark). Under 50% H_2-mixed gas, the H_2 concentration was maintained at 365 ± 5 μM and the O_2 concentration was maintained at 245 ± 5 μM. Under N_2-mixed gas, the H_2 concentration was undetectable and the O_2 concentration was maintained at 250 ± 5 μM.

Lipid extraction

After incubation of cells under a mixed-gas atmosphere, the culture medium was aspirated from the dish, and cells were washed twice with cold phosphate-buffered saline at 4°C and treated with 200 μL of methanol and then with 600 μL of chloroform. Cell extracts were collected and stored at –80°C for definition of changes in major lipid components by using liquid chromatography-high-resolution mass spectrometry.

Liquid chromatography-high-resolution mass spectrometry analysis of lipids

A liquid chromatography system (UltiMate 3000 Rapid Separation LC; ThermoFisher Scientific, Waltham, MA, USA) was used. An Acquity UPLC Peptide BEH C18 column (50 mm × 2.1 mm; 1.7 μm; 130 Å; Waters, Milford, MA, USA) was used for separation. A two-solvent gradient of mobile phase A and mobile phase B was utilized, where mobile phase A was a 6:4 (v/v) mixture of acetonitrile:water containing 10 mM ammonium formate and 0.1% formic acid, and mobile phase B was a 9:1 (v/v) mixture of isopropanol:acetonitrile containing 10 mM ammonium formate and 0.1% formic acid. Measurements were performed with a column flow rate of 0.25 mL/min, a column temperature of 45°C, an autosampler temperature of 5°C, and a sample injection volume of 5 μL. The gradient conditions were set to 0 minute, 0% B; 1 minute, 0% B; 5 minutes, 40% B; 7.5 minutes, 64% B; 12.0 minutes, 64% B; 12.5 minutes, 82.5% B, 19 minutes, 85% B; 25 minutes, 95% B; 25.1 minutes, 0% B; and 30 minutes, 0% B.

An Orbitrap Fusion Lumos mass spectrometer equipped with heated electrospray ionization (ThermoFisher Scientific) was used. In untargeted analysis, the mass spectrometer was set to full mass spectrometry (MS) scan mode (resolution 120,000) and then to data-dependent MS/MS scan mode (resolution 15,000). The automatic gain control target values were set to 4e5 and 5e4 for MS and MS/MS scans, respectively. The maximum injection time was 50 and 80 ms for full MS and MS/MS scans, respectively. The higher-energy collisional dissociation was set to gradual collision energy of 30 ± 10% in negative ion mode and 27 ± 5% in positive ion mode. The quadrupole isolation window was set to 1.0 Da. The ion source settings were spray voltage = 3.2 kV (both pole and cathode of electrospray ionization), vaporizer = 275°C, ion transfer tube = 300°C, radio frequency lens = 40%, sheath gas = 40, auxiliary gas = 10, and sweep gas = 1.

Thermo Scientific Lipid Search software version 4.2 and a database based on MASS LIST were used to identify and quantitatively determine lipids. Substance candidates were estimated using lipid precursor ions and MS/MS fragment ions measured within an error range of ±5 ppm from individual data files, and the predicted material ratios were estimated using the simultaneously obtained peak areas.

Measurement of metabolites

Culture medium in Φ10 cm dishes was aspirated and cells were washed twice with 5% mannitol solution (10 mL followed by 2 mL). Cells were treated with 800 μL of methanol and left for 30 seconds to inactivate enzymes. The cell extract was then treated with 550 μL of Milli-Q water containing internal standards (H3304-1002; Human Metabolome Technologies, Tsuruoka, Japan) and left for another 30 seconds. The extract was centrifuged (2300 × *g* at 4°C for 5 minutes) and then 800 μL of the upper aqueous layer was centrifugally filtered (9100 × *g*

at 4°C for 120 minutes) through a Millipore 5-kDa cutoff filter (UltrafreeMC-PLHCC, Human Metabolome Technologies) to remove macromolecules. The filtrate was centrifugally concentrated and re-suspended in 50 μL of ultrapure water. The obtained samples were sent to Human Metabolome Technologies for analysis by capillary electrophoresis time-of-flight mass spectrometry.

Immunocytochemistry

Immunocytochemistry was performed as previously described.[14] Cells were fixed with phosphate-buffered saline containing 4% paraformaldehyde, permeabilized with 0.2% Triton X-100, blocked with 3% bovine serum albumin, and incubated with the following primary antibodies over night at 4°C: an anti-Rab5 (EE marker) rabbit polyclonal antibody (1:200; Cell Signaling, Danvers, MA, USA, Cat# 3547, RRID:AB_2300649), an anti-Rab7 (LE marker) rabbit polyclonal antibody (1:200; Cell Signaling, Cat# 9367, RRID:AB_1904103), and an anti-GM130 (Golgi marker) mouse monoclonal antibody (1:200; Abcam, Cambridge, UK, Cat# ab169276, RRID:AB_2894838). After washing, cells were further incubated with Alexa Fluor 488-labeled goat anti-rabbit IgG (1:500; Cell Signaling, Cat# 4412, RRID:AB_1904025) and Alexa Fluor 647-labeled goat anti-mouse IgG (1:500; ThermoFisher Scientific, Cat# A21236, RRID:AB_2535805) secondary antibodies for 60 minutes at room temperature. After staining, cells were counterstained with Hoechst 33342 (1:1000; Nacalai, Kyoto, Japan) and imaged using a laser scanning confocal microscope (TCS SP8; Leica, Wetzlar, Germany). For Rab11 (RE marker) staining, cells were fixed with 4% paraformaldehyde for 15 minutes and 10% trichloroacetic acid at 4°C for 15 minutes, permeabilized with 0.2% Triton X-100, blocked with 3% bovine serum albumin, and incubated with an anti-Rab11 rabbit polyclonal antibody (1:200; Cell Signaling, Cat# 5589, RRID:AB_10693925) over night at 4°C. After washing, cells were processed as described above. To quantify the vesicle area, the number and size of vesicles were quantified using ImageJ 2.1.0 (National Institutes of Health, Bethesda, MD, USA).

Western blot

Cells were homogenized in radioimmunoprecipitation assay buffer (50 mM Tris–HCl (pH 8.0), 1% octylphenoxypolyethoxyethanol, 0.1% sodium dodecyl sulfate, 0.5% sodium deoxycholate, 150 mM NaCl, 1 mM ethylenediaminetetraacetic acid) containing protease inhibitors (cOmplete, Roche Diagnostics, Rotkreuz, Switzerland) and centrifuged (15,000 × *g* at 4°C for 20 minutes). The supernatant was collected and stored at –80°C. Heat-denatured proteins (5 μg per lane) were separated on a 10% acrylamide gel and electrotransferred onto a polyvinylidene fluoride membrane. The membranes were blocked with skim milk and incubated at 4°C overnight with primary polyclonal rabbit antibodies against Rab5 (1:2000; Cell Signaling, Cat# 3547, RRID:AB_2300649), Rab7 (1:2000; Cell Signaling, Cat# 9367, RRID:AB_1904103), and Rab11 (1:2000; Cell Signaling, Cat# 5589, RRID:AB_10693925). After washing, membranes were incubated with peroxidase-conjugated anti-rabbit IgG (1:10,000; Jackson, West Grove, PA, USA, Cat# 111-035-144, RRID:AB_2307391) at room temperature for 1 hour. Protein bands were detected with an enhanced chemiluminescence kit (ECL Prime; GE Healthcare, Chicago, IL, USA) and visualized with a CCD imaging system (FUSION Solo S; Vilber Lourmat, Marne-la-Vallée, France). As a normalization control, the membranes were stripped and incubated with a polyclonal rabbit antibody against glyceraldehyde 3-phosphate dehydrogenase (1:2500, Cell Signaling, Cat# 2118, RRID:AB_561053).

CTxB and Tfn uptake assay

Immediately after exposure of cells in 96-well plates to appropriate mixed gas, the culture medium was replaced by Dulbecco's modified Eagle medium containing 312.5 ng/mL Alexa Fluor 555-conjugated CTxB (ThermoFisher Scientific) or 25 μg/mL Alexa Fluor 555-conjugated Tfn (ThermoFisher Scientific) warmed to 37°C. Cells treated with the endocytosis inhibitors wortmannin (5 μM; Adipogen, San Diego, CA, USA) and methyl-β-cyclodextrin (1 mM; Sigma-Aldrich, St. Louis, MO, USA) for 1 hour were used as positive controls. Cells were further incubated in a conventional 5% CO_2 incubator at 37°C for 5 or 10 minutes, fixed with 4% paraformaldehyde, rinsed three times with phosphate-buffered saline, counterstained with Hoechst 33342 for 1 hour, and rinsed twice with Tris-buffered saline containing 0.1% Tween-20. Plates were scanned using a microplate fluorometer (Nivo, PerkinElmer, MA, USA) with excitation and emission wavelengths of 546 and 580 nm, respectively. Cells were further imaged using IN Cell Analyzer 6000 (GE Healthcare).

Statistical analysis

Statistical analyses were performed using JMP8 (SAS, Cary, NC, USA) and Prism 8 (GraphPad Software, San Diego, CA, USA). All values are presented as the mean ± standard deviation (SD). Significance was determined by a one-way analysis of variance with Tukey's *post hoc* test. $P < 0.05$ was considered significant. Principal component analysis (PCA) for lipids was performed using RStudio ver.1.4 (RStudio, Boston, MA, USA). PCA and hierarchical cluster analysis for metabolites were performed using SampleStat ver.3.14 and PeakStat ver.3.18 (both from Human Metabolome Technologies), respectively.

RESULTS

Effects of short exposure to H_2 on lipid composition

After exposure of cultured SH-SY5Y cells to 50% H_2 gas at 37°C for 1 and 6 hours, cellular lipids were extracted with methanol and chloroform. To define changes in major lipid components, we used liquid chromatography-high-resolution mass spectrometry, which is a powerful tool to examine the lipidomic signatures of biological samples in an unbiased manner. We simultaneously quantified 15 lipid classes, including phospholipids, gangliosides, and diacylglycerol (DAG), normalized to the cell number (**Table 1**). PCA revealed clear clustering of lipid species in H_2-treated and control cells (**Figure 1A**). Based on the loading values, PE (–0.398), CL (–0.383), PI (–0.372), PS (–0.361) and DAG (–0.384) were the major contributors for component 1,

Table 1: Peak areas of lipid classes by liquid chromatography-high-resolution mass spectrometry method

				P-value		
Label	**Control**	**H_2 1 h**	**H_2 6 h**	**Control *vs.* H_2 1 h**	**H_2 1 h *vs.* H_2 6 h**	**Control *vs.* H_2 6 h**
CL	34797±5152	46547±5263	34486± 3451	0.0502	*0.0455	0.9964
DAG	153111±50138	228027±6276	145132±22498	0.0722	0.05	0.9534
GM2	19388±510	19657±603	19143± 2368	0.9716	0.9016	0.9765
GM3	3996±279	3867±243	3756± 56	0.7536	0.8117	0.4167
LPA	543±78	663±107	586± 84	0.304	0.5783	0.832
LPC	30992±2824	35382±811	37788± 2109	0.0928	0.3936	0.0170
LPE	16943±2873	18577±351	16677±748	0.4223	0.4223	0.9807
LPI	2624±139	2740±211	3104±640	0.9332	0.5363	0.3644
PA	471±43	597±97	578±129	0.3148	0.9686	0.4159
PC	1421204±120704	1430958±62686	1458470±81747	0.9907	0.929	0.8748
PE	474684±27714	537107±27964	468650± 12017	0.0417	0.0287	0.9485
PG	27604±2704	28801±1872	29601±2110	0.7993	0.9028	0.5568
PI	575658±24120	643394±31431	577475±20788	0.0420	0.0466	0.9959
PS	268589±11820	302411±19287	268642±14108	0.0801	0.0805	1
SM	85109±12559	81741±6178	90369±1447	0.8704	0.445	0.7206
SUM	3115712±74922	3380470±160544	3154457±119447	0.0867	0.1415	0.9227

Note: Data are expressed as mean ± SD (n = 3), and were analyzed by one-way analysis of variance with Tukey's *post hoc* test. CL: Cardiolipin; DAG: diacylglycerol; GM2: ganglioside; GM3: glycosphingolipid; H_2: molecular hydrogen; LPA: lysophosphatidic acid; LPC: lysophosphatidylcholine; LPE: lysophosphatidylethanolamine; LPI: lysophosphatidylinositol; PA: phosphatidic acid; PC: phosphatidylcholine; PE: phosphatidylethanolamine; PG: phosphatidylglycerol; PI: phosphatidylinositol; PS: phosphatidylserine; SM: sphingomyelin; SUM: total value.

whereas phosphatidylglycerol (PG, –0.470), PC (–0.423) and sphingomyelin (SM, –0.396) were the main contributors for component 2.

The levels of PE, CL and PI were significantly higher in H_2-1 hour treated cells than in control cells and H_2-6 hours treated cells (**Figure 1B**), whereas the total sum of all lipids per cell did not differ. H_2-treated cells also tended to have a transiently increased level of PS. However, H_2 exposure did not change the proportion of PC, which is the most abundant phospholipid, but significantly increased that of lysophosphatidylcholine, which is mainly derived from turnover of PC, in H_2-6 hours treated cells (**Table 1**). In addition, there were no significant differences in free fatty acids or triglycerides between the groups (data not shown). CL is uniquely synthesized in mitochondria, predominantly localizes to the inner mitochondrial membrane (IMM), and cooperates with PE to maintain mitochondrial activity.[21] H_2-treated cells tended to have an increased level of DAG (**Figure 1B**), which is generated via dephosphorylation of phosphatidic acid and utilized to synthesize PC and PE.

To assess the effects of H_2 exposure on the degree of unsaturation and length of hydrocarbon chains, we compared all PI and PS species with the same amount of unsaturation or the same total carbon chain length. Neither the level of unsaturation nor the length of hydrocarbon chains increased upon H_2 exposure for 1 hour (**Figure 2**). These results indicate that the level of almost every PI and PS species was elevated upon H_2 exposure.

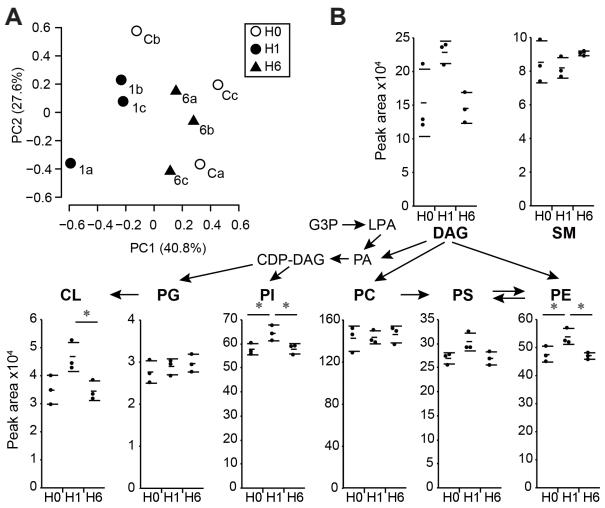

Figure 1: Changes to lipid composition induced by H_2 in SH-SY5Y cells.
Note: (A) A plot of principal component 1 (PC1) versus principal component 2 (PC2) based on the results of principal component analysis. Percentages in parentheses indicate the contribution of each principal component. (B) Peak areas of the main phospholipids and DAG. Synthetic pathway for phospholipids. H_2 exposure significantly increased the levels of PE, CL, PI, and DAG. Data are expressed as mean ± SD (n = 3). *P<0.05 (one-way analysis of variance with Tukey's *post hoc* test). H0, H1 and H6 indicate cells incubated with 50% H_2 gas for 0, 1 and 6 hours, respectively. CL: Cardiolipin; DAG: diacylglycerol; H_2: molecular hydrogen; PE: phosphatidylethanolamine; PI: phosphatidylinositol.

Metabolomic changes induced by H_2 exposure

The compositions of CL and PE in mitochondria affect respiratory chain function and modify energy metabolism. Indeed, we previously observed that H_2 exposure significantly changes the mitochondrial membrane potential and cellular O_2 consumption accompanied by a reduction in glutathione.[14] To determine early H_2-induced changes, SH-SY5Y cells cultured in the presence of H_2 for 1 and 6 hours were analyzed by metabolomics. We selected 116 metabolites (52 cations and 64 anions) that contribute to the glycolytic system, the pentose phosphate pathway, the tricarboxylic acid cycle, the urea circuit, the polyamine and creatine metabolic pathways, the purine metabolic pathway, the glutathione metabolic pathway, the nicotinamide metabolic pathway, the choline metabolic

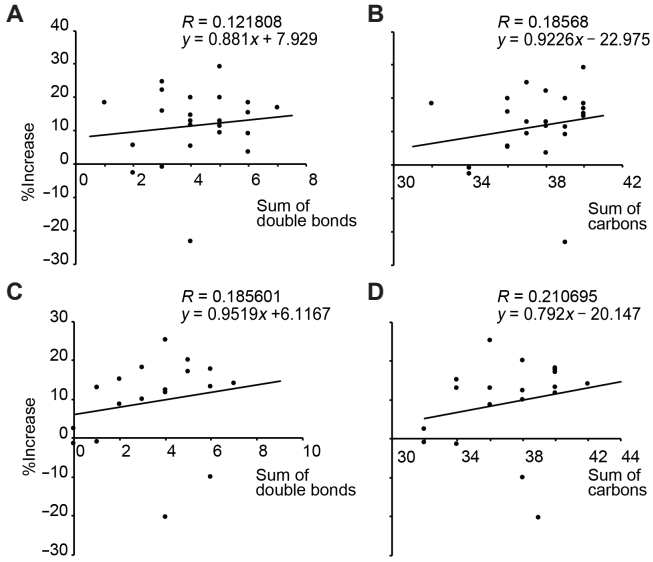

Figure 2: Effects of H_2 on the degree of unsaturation and length of hydrocarbon chains in SH-SY5Y cells.

Note: (A–D) Scatterplots between the increase in PI species (A, B) and PS species (C, D) after H_2 exposure for 1 hour (normalized to control) *vs.* the sum of double bonds (A, C) and the sum of carbons (B, D). Linear regression line and Pearson's *R* value are shown in each plot (n = 3). H_2: Molecular hydrogen; PI: phosphatidylinositol; PS: phosphatidylserine.

pathway, and various amino acid metabolic pathways. PCA comparing the overall metabolomics profiles showed excellent clustering of metabolomic changes in control cells and cells treated with H_2 for 1 and 6 hours, demonstrating that H_2 exposure led to a distinct metabolic profile (**Figure 3A**).

A heat representation of the metabolomic profiles analyzed by hierarchical clustering is provided in **Figure 3B**. A number of characteristic changes were noted in H_2-exposed cells. The levels of the majority of metabolites were decreased after exposure to H_2 for 1 hour. These included glycolytic metabolites (fructose 6-phosphate, fructose 1,6-bisphosphate, glyceraldehyde 3-phosphate, dihydroxyacetone phosphate, glycerol 3-phosphate, 3-phosphoglyceric acid, 2-phosphoglyceric acid, pyruvic acid, and lactic acid) (**Figure 3C**), tricarboxylic acid cycle metabolites (citric acid, 2-oxoglutaric acid, succinic acid, and malic acid) (**Figure 3D**), and some amino acids (Gly, Met, Tyr, and Val). Fructose 1,6-bisphosphate is metabolized into dihydroxyacetone phosphate and glyceraldehyde 3-phosphate by aldolase, and levels of these three metabolites were markedly decreased. The reduced nicotinamide adenine dinucleotide level was significantly decreased and the adenosine triphosphate level tended to be decreased in cells exposed to H_2 for 1 hour (**Figure 3E**). After 6 hours, the levels of many of these downregulated metabolites, including reduced nicotinamide adenine dinucleotide and adenosine triphosphate, were restored to those in control cells; however, the levels of pyruvate and tricarboxylic acid cycle metabolites remained decreased. While the reduced/oxidized nicotinamide adenine dinucleotide ratio was unchanged after exposure to H_2 for 1 or 6 hours, the lactate/pyruvate and malate/Asp ratios were significantly decreased. These results indicate that although H_2 transiently inhibited overall metabolism, it continuously inhibited energy metabolism in mitochondria.

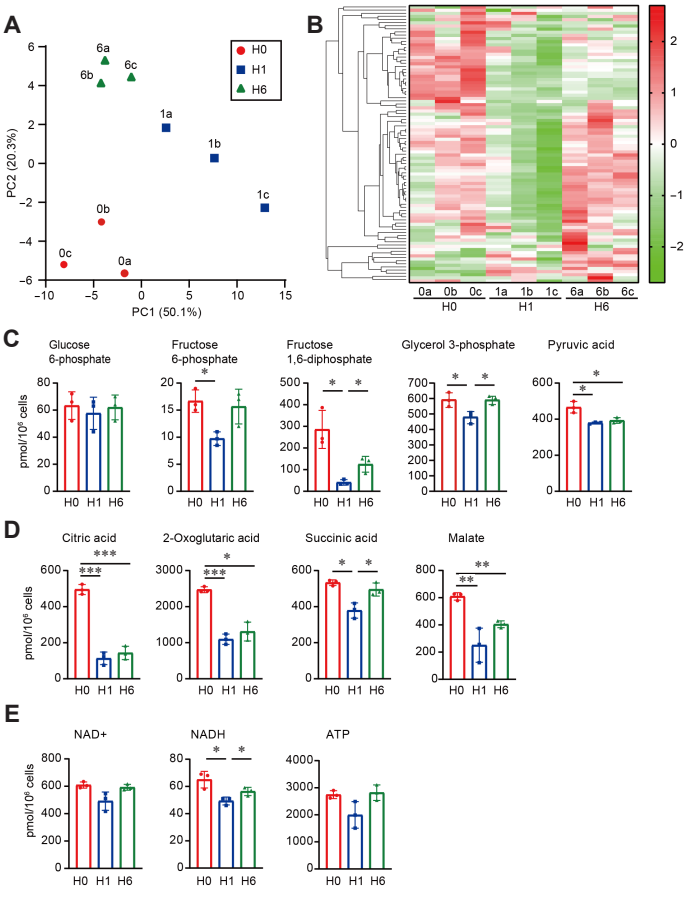

Figure 3: Metabolomic changes in SH-SY5Y cells induced by H_2.

Note: (A) A plot of principal component 1 (PC1) versus principal component 2 (PC2) based on the results of PCA. Percentages in parentheses indicate the contribution of each principal component. (B) Heat map representation of metabolomic profiles analyzed by hierarchical clustering. Tree diagrams represent correlations between peaks. Darker green indicates lower than average and darker red indicates higher than average. (C–E) Specific metabolic changes in glycolysis (C), the tricarboxylic acid cycle (D) and the energy status (E) induced by exposure to H_2 for 0, 1, and 6 hours. Data are mean ± SD (n = 3). *P < 0.05, **P < 0.01, ***P < 0.001 (one-way analysis of variance with Tukey's *post hoc* test). H0, H1, and H6 indicate cells incubated with 50% H_2 gas for 0, 1, and 6 hours, respectively. H_2: Molecular hydrogen.

Effects of short exposure to H_2 on glutathione level

Noteworthy, the metabolomic profiles revealed the decrease in glutathione level accompanied by a reduction in the glutathione redox ratio after exposure to H_2 for 1 hour, suggesting that culture of cells in the presence of H_2 for 1 hour is sufficient to induce oxidative stress (**Figure 4**). However, the glutathione level was not decreased after exposure to H_2 for 6 hours, indicating that H_2 transiently induces oxidative stress.

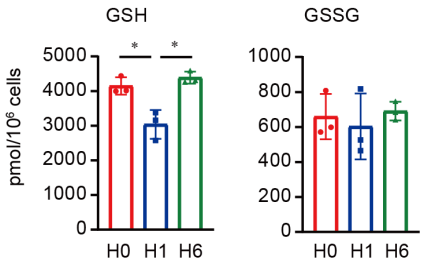

Figure 4: Transient oxidative stress in SH-SY5Y cells induced by H_2.
Note: Metabolic changes in glutathione (GST and GSSG) induced by exposure to H_2 for 0, 1, and 6 hours (H0, 1, 6). Data are expressed as mean ± SD (n = 3). *P<0.05 (one-way analysis of variance with Tukey's *post hoc* test). GSSG: Glutathione disulfide; GST: glutathione S-transferases; H_2: molecular hydrogen.

Effects of short exposure to H_2 on endocytosis and endosomal transport

Phosphorylated forms of PI, phosphoinositides, play important roles in lipid signaling, cell signaling and membrane trafficking.[22] PS is more abundant in the plasma membrane and endosomes than in the endoplasmic reticulum, where it is synthesized, and facilitates endocytosis.[22] We then speculated that H_2 treatment affects endocytosis and vesicular transport. We first observed the morphology of endosomes in SH-SY5Y cells exposed to H_2 for 1 hour. Confocal microscopy of fixed cells immunostained with antibodies against endosomal markers showed that areas positive for the EE marker Rab5 and the RE marker Rab11 were significantly larger in H_2-exposed cells than in control cells (**Figure 5A**, **B**, **E**, and **F**), whereas the area positive for the LE marker Rab7 was significantly smaller (**Figure 5C** and **D**). On the other hand, immunoblotting showed that exposure to H_2 for 1 hour did not affect the protein levels of Rab5, Rab7, and Rab11 (**Figure 5G** and **H**).

To investigate the effects of H_2 on endocytosis, we examined cellular uptake of CTxB and Tfn. At 5 and 10 minutes after addition of fluorescently labeled CTxB or Tfn, uptake of these two proteins was unaffected in cells exposed to H_2 for 1 hour, but was suppressed in cells treated with the endocytosis inhibitors methyl-β-cyclodextrin and wortmannin (data not shown). Next, we investigated the effects of H_2 on vesicular transport. CTxB is trafficked sequentially from the plasma membrane to EEs and then to REs and finally to the Golgi body.[24] We examined the intracellular localization of fluorescently labeled CTxB at 5 min after its addition (**Figure 6A–D**). The percentage of CTxB that colocalized with Rab5-positive EEs was unaffected in cells exposed to 50% H_2 for 1 hour. On the other hand, a portion of CTxB colocalized with Rab11-positive REs around the Golgi body in control cells and this localization was significantly reduced in H_2-exposed cells. The percentage of CTxB that localized around the Golgi body was significantly lower in 50% H_2-exposed cells than in control cells at 5 minutes, but not at 10 minutes, after addition of CTxB (**Figure 6E**). These results strongly suggest that H2 exposure delayed endosomal transport. Notably, the H_2-induced delay in endosomal transport was dose-dependent, and exposure to 2% H_2 was sufficient to decrease CTxB accumulation around the Golgi body.

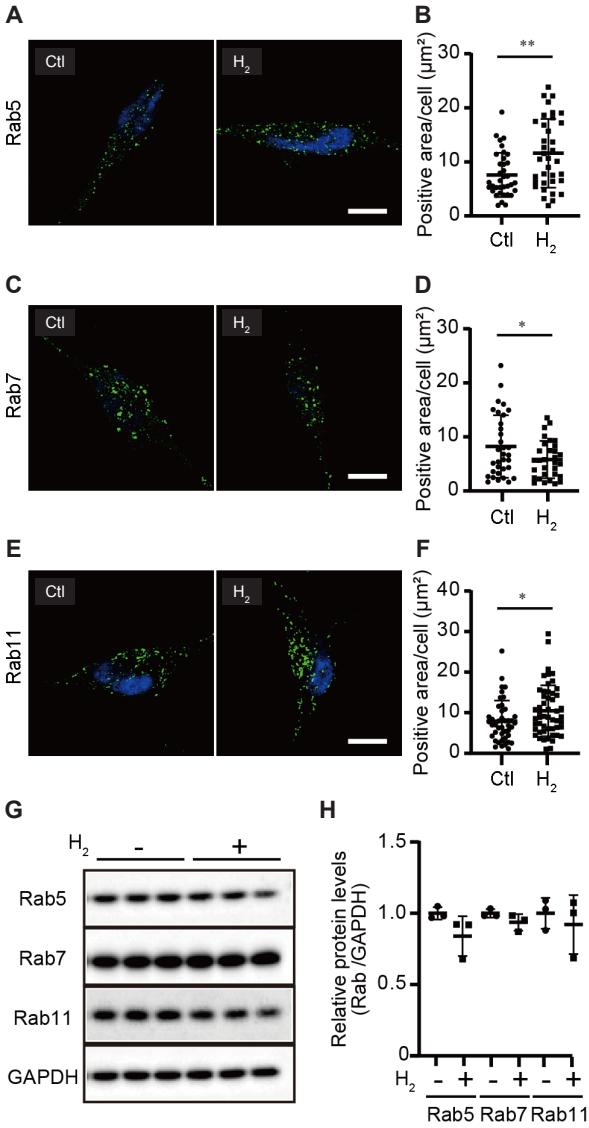

Figure 5: Changes in endosomal area in SH-SY5Y cells induced by H_2.
Note: (A–F) Immunocytochemical analysis of cells treated with (H_2) or without (Ctl) 50% H_2 gas for 1 hour. Cells were stained with antibodies against the early endosome marker Rab5 (A, B), the late endosome marker Rab7 (C, D), and the recycling endosome marker Rab11 (E, F) (green: Alexa Fluor 488), and counterstained with Hoechst 33342 (blue). The area positive for each marker per cell (B, D, F) are shown. (G, H) Immunoblotting of cells treated with or without 50% H_2 using antibodies against Rab5, Rab7, Rab11, and glyceraldehyde 3-phosphate dehydrogenase (GAPDH) as an internal control. (H) Relative protein expression levels were quantified. Data are expressed as mean ± SD (n = 3). *P<0.05, **P<0.01 (one-way analysis of variance with Tukey's *post hoc* test). Ctl: Control; H_2: molecular hydrogen.

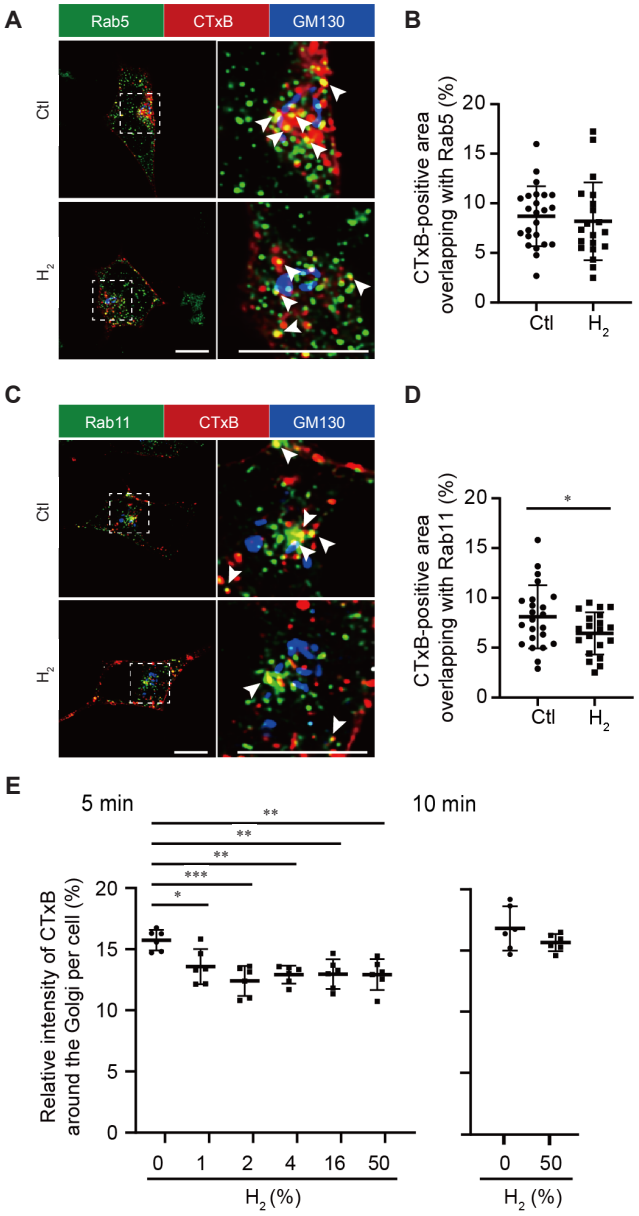

Figure 6: Delay of endosomal transport in SH-SY5Y cells induced by H_2.
Note: (A–D) Differential accumulation of cholera toxin B (CTxB) in endosomes. At 5 minutes after addition of Alexa Fluor 555-conjugated CTxB, cells that had been preincubated with (H_2) or without (Ctl) 50% H_2 for 1 hour were stained with an early endosome (EE)-specific anti-Rab5 (A) or recycling endosome (RE)-specific anti-Rab11 (C) antibody and a Golgi body-specific anti-GM130 antibody. CTxB partially colocalized with EEs and REs (arrowheads). The area of CTxB that colocalized with the Rab5-positive (B) or Rab11-positive (D) region in each cell was quantified. Scale bars: 10 μm. (E) Quantitative analysis of the relative fluorescence intensity of CTxB around the Golgi body in cells treated with different concentrations of H_2. At the indicated timepoint after addition of Alexa Fluor 555-conjugated CTxB, cells were fixed. Values are the fluorescence intensity of Alexa Fluor 555-conjugated CTxB around the Golgi body relative to the fluorescence intensity in the whole cell. Each dot is the average of values from 10–16 cells in a well. Data are expressed as mean ± SD ($n = 5$). *$P < 0.05$, **$P < 0.01$, ***$P < 0.001$ (one-way analysis of variance with Tukey's *post hoc* test). Ctl: Control; H_2: molecular hydrogen.

Discussion

Short exposure to H_2 transiently increased the levels of phospholipids, including CL, PE and PI, in cultured neuroblastoma cells (**Figure 1**). Synthesis of all classes of phospholipids begins with two common precursors, phosphatidic acid and DAG, largely in the endoplasmic reticulum.[25] H_2 also transiently increased the level of DAG. However, metabolomics revealed that the level of glycerol 3-phosphate, a key precursor of glycerolipids including triacylglycerol, DAG and phospholipids, was significantly and transiently downregulated by H_2-exposure (**Figure 3**). We can speculate the possibility that short exposure of H_2 disturbs the phospholipid catabolic pathway including phospholipases. The majority of these enzymes are soluble and interact with the membrane in a transient fashion.[26] Further studies are needed to elucidate the molecular mechanisms underlying the increase of phospholipids by H_2 exposure.

The levels of CL and PE, whose levels were significantly and transiently increased by H_2 exposure (**Figure 1**), are significantly higher in mitochondria, particularly the IMM, than in other organelles.[27] CL synthetase catalyzes formation of CL from PG and cytidine diphosphate-DAG in the IMM. Mitochondrial biogenesis factors regulate expression and activities of CL synthesizing enzymes.[28] PE is synthesized in the endoplasmic reticulum via the cytidine diphosphate-ethanolamine pathway. Short exposure to H_2 tended to increase the PS level (**Figure 1**). PS is also an important precursor of mitochondrial PE, which is produced by mitochondrial PS decarboxylase in the IMM.[29] Inhibition of PS decarboxylase alters the mitochondrial membrane composition and induces bioenergetic impairment.[30] CL, PE and PS can impact mitochondrial function by forming molecular interactions with each other and with target proteins or by modulating the bulk properties of membranes due to their propensity to form non-bilayer structures. Therefore, we speculated that the H_2-induced increases in CL, PE and PS affect energy metabolism.

Our metabolomic data showed that H_2 exposure for 1 hour transiently inhibited overall metabolism, whereas it was almost recovered at 6 hours (**Figure 3**). We then consider that H_2-induced transient and reversible increase in phospholipids is related to this metabolic disturbance. Noteworthy, cells were still exposed with 50% H_2 at 6 hours. One possible reason for the transient effect is that the physiological function of H_2 is associated with its non-homogeneous distribution immediately after H_2 addition, which is rapidly lost due to the high diffusivity of H_2. This possibility is supported by the finding of Ito et al.[31] that intermittent exposure to H_2 gas prevents Parkinson's disease in rats, whereas continuous exposure does not. It is known that structural and dynamic changes in cell membrane properties are induced by non-homogeneous distribution of gaseous molecules. For example, xenon atoms, volatile anesthetic gas, preferentially localize in the hydrophobic core of the lipid bilayer, inducing increases in the area per lipids and bilayer thickness.[32] We found that energy metabolism in mitochondria was continuously inhibited at least until 6 hours. It suggested that H_2 exposure induces more stress in the mitochondria.

H_2 exposure for 1 hour significantly decreased accumulation of glutathione and reduced the glutathione redox ratio (**Figure 4**). Activation of nuclear factor-erythroid factor 2-related factor 2 (Nrf2) induces glutathione synthesis. We previously reported that exposure of SH-SY5Y cells to H_2 enhances production of mitochondrial superoxide accompanied by translocation of Nrf2 into the nucleus and elevated expression of antioxidative enzymes that are regulated by Nrf2, suggesting

that H_2-induced mitochondrial oxidative stress activates Nrf2.[14] We also demonstrated that the Keap1–Nrf2, which reduces oxidative stress, is activated in the liver of mice treated with lipopolysaccharide after H_2 administration.[8] Addition of 2% H_2 gas suppresses pulmonary disorders caused by 98% oxygen load in normal mice, but not in Nrf2-knockout mice.[33] Our results indicate the possibility that transient H_2-induced increase in phospholipids and inhibition of overall metabolism elicits antioxidative effects by activating the Keap1–Nrf2 pathway.

Diverse cellular processes including endocytosis, phagocytosis, and autophagy are regulated by PI 3-phosphate, which is mainly generated by the class III phosphoinositide 3-kinase vacuolar protein sorting 34.[34] Phosphoinositides including PI 3-phosphate are synthesized from PI, whose level was significantly and transiently increased by H_2 exposure (**Figure 1**). Therefore, we speculated that changes in lipid composition upon H_2 exposure might affect endocytosis and endosomal transport. On the other hand, in the presence of catalyst, hydrogenation reduces double bonds in hydrocarbons and modulates membrane fluidity. However, H_2 exposure did not affect the degree of unsaturation and length of hydrocarbon chains in PI and PS (**Figure 2**).

We then found that H_2 exposure increased the areas of Rab5-positive EEs and Rab11-positive REs, but decreased that of Rab7-positive LEs (**Figure 5**). The small GTPase Rab5 participates in recruitment of vacuolar protein sorting 34 to EEs,[35] and vacuolar protein sorting 34 negatively regulates Rab5 during endosome maturation,[36] which may be associated with the effects of H_2 exposure on Rab5-positive EEs. However, H_2 suppressed endosomal trafficking (**Figure 6**), but did not affect clathrin-dependent or -independent endocytosis (data not shown). CTxB is trafficked sequentially from the plasma membrane to Rab5-positive EEs and then to Rab11-positive REs and finally to the Golgi body.[24] H_2 exposure delayed accumulation of CTxB in REs, which are typically located deep within cells and centered around the microtubule-organizing center. H_2 exposure may delay transport of CTxB from EEs to REs. Noteworthy, exposure to 2% H_2 was sufficient to delay accumulation of CTxB in REs. These results are consistent with those obtained in many animal models and human clinical trials, which reported that inhalation of ~2% H_2 gas is effective and sufficient to cure diseases.[1,37,38]

Only a few studies have reported molecules upon which H_2 acts directly. For further medical applications of H_2, it is necessary to identify the biomolecule(s) upon which it acts. The present study showed that short exposure to H_2 transiently modifies cellular lipid contents. However, it remains unclear whether H_2 is directly or indirectly involved in lipid metabolism. We previously reported that helium instead of H_2 did not protect ischemia-reperfusion injury in the kidney.[39] However, other noble gases, argon and xenon, have been reported to mitigate cell death in cellular experiments, whereas helium has not.[40-42] Interestingly, several studies have indicated that inhaled anesthetics including xenon directly perturb the fluidity of membrane lipids and alter lipid contents.[17,32,43] These and then, H_2 may act on lipids through a mechanism similar to that of inhaled anesthetics. We speculate that H_2-induced modification of lipid composition depresses endosomal transport and energy production concomitant with enhancement of oxidative stress. On the other hand, maintenance of the membranous system including regulation of plasma membrane and vesicular transport consumes about 30% of cellular energy,[44] indicating that the physiological changes presented here are interrelated.

In this study, we found that H_2 exposure transiently and reversibly increased the level of several phospholipids and slightly disturbed endosomal transport. Metabolomic data also indicate that short exposure to H_2 transiently suppressed metabolic pathways involved in energy production and concomitantly increased oxidative stress, which may trigger a protective adaptive response.

Author contributions

IO originally designed the study. MIketani, IS, and YF performed experiments and analyzed and interpreted data. MIketani and IO performed statistical analyses. MIto supervised the study. MIketani, IS and IO wrote the manuscript, and IO edited the manuscript. All authors read and approved the final manuscript.

Conflicts of interest

Iwao Sakane is an employee of Central Research Institute, ITO EN Ltd., Shizuoka, Japan. The authors declare that they have no conflicts of interest with the contents of this article.

References

1. Ohsawa I, Ishikawa M, Takahashi K, et al. Hydrogen acts as a therapeutic antioxidant by selectively reducing cytotoxic oxygen radicals. *Nat Med.* 2007;13:688-694.
2. Slezák J, Kura B, Frimmel K, et al. Preventive and therapeutic application of molecular hydrogen in situations with excessive production of free radicals. *Physiol Res*. 2016;65 Suppl 1:S11-28.
3. Yoritaka A, Takanashi M, Hirayama M, Nakahara T, Ohta S, Hattori N. Pilot study of H therapy in Parkinson's disease: a randomized double-blind placebo-controlled trial. *Mov Disord*. 2013;28:836-839.
4. Nishimaki K, Asada T, Ohsawa I, et al. Effects of molecular hydrogen assessed by an animal model and a randomized clinical study on mild cognitive impairment. *Curr Alzheimer Res*. 2018;15:482-492.
5. Iketani M, Ohsawa I. Molecular hydrogen as a neuroprotective agent. *Curr Neuropharmacol.* 2017;15:324-331.
6. Qiu X, Li H, Tang H, et al. Hydrogen inhalation ameliorates lipopolysaccharide-induced acute lung injury in mice. *Int Immunopharmacol.* 2011;11:2130-2137.
7. Xie K, Yu Y, Huang Y, et al. Molecular hydrogen ameliorates lipopolysaccharide-induced acute lung injury in mice through reducing inflammation and apoptosis. *Shock.* 2012;37:548-555.
8. Iketani M, Ohshiro J, Urushibara T, et al. Preadministration of hydrogen-rich water protects against lipopolysaccharide-induced sepsis and attenuates liver injury. *Shock.* 2017;48:85-93.
9. Kajiya M, Sato K, Silva MJ, et al. Hydrogen from intestinal bacteria is protective for Concanavalin A-induced hepatitis. *Biochem Biophys Res Commun.* 2009;386:316-321.

10. Kajiya M, Silva MJ, Sato K, Ouhara K, Kawai T. Hydrogen mediates suppression of colon inflammation induced by dextran sodium sulfate. *Biochem Biophys Res Commun*. 2009;386:11-15.
11. Shen NY, Bi JB, Zhang JY, et al. Hydrogen-rich water protects against inflammatory bowel disease in mice by inhibiting endoplasmic reticulum stress and promoting heme oxygenase-1 expression. *World J Gastroenterol.* 2017;23:1375-1386.
12. Buxton GV, Greenstock CL, Helman WP, Ross AB. Critical review of rate constants for reactions of hydrated electrons, hydrogen atoms and hydroxyl radicals (•OH/•O^- in Aqueous Solution. *J Phys Chem Ref Data.* 1988;17:513-886.
13. Yoshii Y, Inoue T, Uemura Y, et al. Complexity of stomach-brain interaction induced by molecular hydrogen in Parkinson's disease model mice. *Neurochem Res*. 2017;42:2658-2665.
14. Murakami Y, Ito M, Ohsawa I. Molecular hydrogen protects against oxidative stress-induced SH-SY5Y neuroblastoma cell death through the process of mitohormesis. *PLoS One.* 2017;12:e0176992.
15. Power GG, Stegall H. Solubility of gases in human red blood cell ghosts. *J Appl Physiol.* 1970;29:145-149.
16. Lee CW, Chiang YL, Liu JT, et al. Emerging roles of air gases in lipid bilayers. *Small.* 2018;14:e1802133.
17. Lerner RA. A hypothesis about the endogenous analogue of general anesthesia. *Proc Natl Acad Sci U S A.* 1997;94:13375-13377.
18. Yonamine R, Satoh Y, Kodama M, Araki Y, Kazama T. Coadministration of hydrogen gas as part of the carrier gas mixture suppresses neuronal apoptosis and subsequent behavioral deficits caused by neonatal exposure to sevoflurane in mice. *Anesthesiology*. 2013;118:105-113.
19. Molliex S, Crestani B, Dureuil B, et al. Effects of halothane on surfactant biosynthesis by rat alveolar type II cells in primary culture. *Anesthesiology.* 1994;81:668-676.
20. Iuchi K, Imoto A, Kamimura N, et al. Molecular hydrogen regulates gene expression by modifying the free radical chain reaction-dependent generation of oxidized phospholipid mediators. *Sci Rep*. 2016;6:18971.
21. Basu Ball W, Neff JK, Gohil VM. The role of nonbilayer phospholipids in mitochondrial structure and function. *FEBS Lett*. 2018;592:1273-1290.
22. Bohdanowicz M, Grinstein S. Role of phospholipids in endocytosis, phagocytosis, and macropinocytosis. *Physiol Rev.* 2013;93:69-106.
23. Grant BD, Donaldson JG. Pathways and mechanisms of endocytic recycling. *Nat Rev Mol Cell Biol.* 2009;10:597-608.
24. Uchida Y, Hasegawa J, Chinnapen D, et al. Intracellular phosphatidylserine is essential for retrograde membrane traffic through endosomes. *Proc Natl Acad Sci U S A*. 2011;108:15846-15851.
25. Tracey TJ, Steyn FJ, Wolvetang EJ, Ngo ST. Neuronal lipid metabolism: multiple pathways driving functional outcomes in health and disease. *Front Mol Neurosci*. 2018;11:10.
26. Horn A, Jaiswal JK. Structural and signaling role of lipids in plasma membrane repair. *Curr Top Membr.* 2019;84:67-98.
27. Daum G. Lipids of mitochondria. *Biochim Biophys Acta.* 1985;822:1-42.
28. Blunsom NJ, Cockcroft S. CDP-diacylglycerol synthases (CDS): gateway to phosphatidylinositol and cardiolipin synthesis. *Front Cell Dev Biol*. 2020;8:63.
29. Kainu V, Hermansson M, Hänninen S, Hokynar K, Somerharju P. Import of phosphatidylserine to and export of phosphatidylethanolamine molecular species from mitochondria. *Biochim Biophys Acta*. 2013;1831:429-437.
30. Bellance N, Furt F, Melser S, et al. Doxorubicin inhibits phosphatidylserine decarboxylase and modifies mitochondrial membrane composition in HeLa cells. *Int J Mol Sci*. 2020;21:1317.
31. Ito M, Hirayama M, Yamai K, et al. Drinking hydrogen water and intermittent hydrogen gas exposure, but not lactulose or continuous hydrogen gas exposure, prevent 6-hydorxydopamine-induced Parkinson's disease in rats. *Med Gas Res.* 2012;2:15.
32. Booker RD, Sum AK. Biophysical changes induced by xenon on phospholipid bilayers. *Biochim Biophys Acta.* 2013;1828:1347-1356.
33. Kawamura T, Wakabayashi N, Shigemura N, et al. Hydrogen gas reduces hyperoxic lung injury via the Nrf2 pathway in vivo. *Am J Physiol Lung Cell Mol Physiol.* 2013;304:L646-656.
34. Burman C, Ktistakis NT. Regulation of autophagy by phosphatidylinositol 3-phosphate. *FEBS Lett.* 2010;584:1302-1312.
35. Murray JT, Panaretou C, Stenmark H, Miaczynska M, Backer JM. Role of Rab5 in the recruitment of hVps34/p150 to the early endosome. *Traffic.* 2002;3:416-427.
36. Law F, Seo JH, Wang Z, et al. The VPS34 PI3K negatively regulates RAB-5 during endosome maturation. *J Cell Sci.* 2017;130:2007-2017.
37. Hayashida K, Sano M, Kamimura N, et al. H(2) gas improves functional outcome after cardiac arrest to an extent comparable to therapeutic hypothermia in a rat model. *J Am Heart Assoc.* 2012;1:e003459.
38. Tamura T, Suzuki M, Hayashida K, et al. Hydrogen gas inhalation alleviates oxidative stress in patients with post-cardiac arrest syndrome. *J Clin Biochem Nutr.* 2020;67:214-221.
39. Fukuda K, Asoh S, Ishikawa M, Yamamoto Y, Ohsawa I, Ohta S. Inhalation of hydrogen gas suppresses hepatic injury caused by ischemia/reperfusion through reducing oxidative stress. *Biochem Biophys Res Commun.* 2007;361:670-674.
40. Spaggiari S, Kepp O, Rello-Varona S, et al. Antiapoptotic activity of argon and xenon. *Cell Cycle*. 2013;12:2636-2642.
41. Jawad N, Rizvi M, Gu J, et al. Neuroprotection (and lack of neuroprotection) afforded by a series of noble gases in an in vitro model of neuronal injury. *Neurosci Lett.* 2009;460:232-236.
42. Rizvi M, Jawad N, Li Y, Vizcaychipi MP, Maze M, Ma D. Effect of noble gases on oxygen and glucose deprived injury in human tubular kidney cells. *Exp Biol Med (Maywood)*. 2010;235:886-891.
43. Liu F, Rainosek SW, Frisch-Daiello JL, et al. Potential adverse effects of prolonged sevoflurane exposure on developing monkey brain: from abnormal lipid metabolism to neuronal damage. *Toxicol Sci*. 2015;147:562-572.
44. Lynch M, Marinov GK. Membranes, energetics, and evolution across the prokaryote-eukaryote divide. *Elife.* 2017;6:e20437.

Date of submission: April 5, 2021
Date of decision: May 13, 2021
Date of acceptance: July 23, 2021
Date of web publication:
December 22, 2022